Hot Isostatic Pressing of Engineered Forms of I-AgZ

Nuclear Technology Research and Development

Prepared for
U.S. Department of Energy
Material Recovery and Waste Form Development Campaign
S. H. Bruffey, J. A. Jordan, R. T. Jubin, M. L. Parks, and T. R. Watkins
Oak Ridge National Laboratory

October 31, 2017
ORNL/SR-2017/707
NTRD-MRWFD-2017-000412

DISCLAIMER

This information was prepared as an account of work sponsored by an agency of the U.S. Government. Neither the U.S. Government nor any agency thereof, nor any of their employees, makes any warranty, expressed or implied, or assumes any legal liability or responsibility for the accuracy, completeness, or usefulness, of any information, apparatus, product, or process disclosed, or represents that its use would not infringe privately owned rights. References herein to any specific commercial product, process, or service by trade name, trade mark, manufacturer, or otherwise, does not necessarily constitute or imply its endorsement, recommendation, or favoring by the U.S. Government or any agency thereof. The views and opinions of authors expressed herein do not necessarily state or reflect those of the U.S. Government or any agency thereof.

SUMMARY

Hot isostatic pressing (HIP) is being considered for direct conversion of ^{129}I-bearing materials to a radiological waste form. The removal of volatile radioactive ^{129}I from the off-gas of a nuclear fuel reprocessing facility will be necessary to comply with regulatory requirements regarding reprocessing facilities sited within the United States, and any iodine-containing media or solid sorbents generated by off-gas abatement will require disposal. Zeolite minerals such as silver-exchanged mordenite (AgZ) have been studied as potential iodine sorbents and will contain ^{129}I as chemisorbed AgI. Oak Ridge National Laboratory (ORNL) has conducted several recent studies on the HIP of both iodine-loaded AgZ (I-AgZ) and other iodine-bearing zeolite minerals.

The goal of these research efforts is to achieve a stable, highly leach resistant material that is reduced in volume as compared to bulk iodine-loaded I-AgZ. Through the use of HIP, it may be possible to achieve this with the addition of little or no additional materials (waste formers). Other goals for the process include that the waste form will be tolerant to high temperatures and pressures, not chemically hazardous, and that the process will result in minimal secondary waste generation.

This document describes the preparation of 27 samples that are distinct from previous efforts in that they are prepared exclusively with an engineered form of AgZ that is manufactured using a binder. Iodine was incorporated solely by chemisorption. This base material is expected to be more representative of an operational system than were samples prepared previously with pure minerals.

The samples prepared can be used to better understand several key parameters of conversion of I-AgZ by HIP. First, the inherent variability in measured properties for identical waste forms produced by HIP of I-AgZ is unknown. To better understand this variability, four sets of small-format replicate samples were prepared. Second, although there has been some limited effort to determine the effect of pressing conditions on sample properties, optimized pressing conditions including pressure, temperature, and time have not yet been established. This sample set will allow for systematic evaluation of pressing conditions using realistic engineered source material (i.e., I-AgZ). Third, the effect of water is not well understood in the HIP process. In this effort, three samples were loaded with iodine and then dried at selected temperatures (150–450°C) to assess the impacts of drying on the produced waste form.

Finally, although HIP is a well-known industrial process commonly performed at large scale, the work reported here on I-AgZ waste forms has been limited to small-format samples. The work reported here included preparation of three samples that were 2× the diameter of the small-format capsules used thus far. These samples are an initial effort to evaluate whether scaled-up HIP of I-AgZ presents any concerns.

One outstanding question pertains to the conversion by HIP of I-AgZ to a radioactive waste form. A key component of any radioactive waste form is its ability to retain the target radionuclide for an extended time. Although durability test methods for homogenous waste forms such as glass are well understood and standardized, similar methods are not yet available for heterogeneous waste forms such as those produced by HIP of I-AgZ. Active efforts to develop new performance testing methods for AgI-containing heterogenous waste forms are intended to account for both chemical dissolution of AgI at exposed waste form surfaces and within grain boundaries of the waste form interior.

This collection of 27 samples will be stored at ORNL and made available for collaborators working on development of performance test methods. Given that these methods are still under development, this document details the preparation of the sample set and serves as a repository of the preliminary characterization efforts for these samples. The densities, mineral phases, and visual appearances of each sample are provided here. It is important that this data and the prepared samples be available and easily referenced in complement of future waste form durability testing.

ORNL will continue to explore the production of large-format capsules to recognize any issues that might arise during scaleup of I-AgZ waste form production by HIP. Future efforts will ensure that current capsule

designs are suitable for scaleup and that sample preparation and encapsulation techniques translate to a larger scale.

CONTENTS

SUMMARY iii

CONTENTS v

FIGURES vi

TABLES viii

ACRONYMS ix

1. INTRODUCTION 1
   1.1 Waste Form Performance Testing 2
   1.2 Objectives and Sample Set 2

2. MATERIALS AND METHODS 4
   2.1 Preparation of I-AgZ 4
   2.2 Encapsulation, Pressing, and Mounting 4

3. ANALYSIS 6
   3.1 Density of Pressed Samples 6
   3.2 Visual Examination 7
   3.3 Optical Microscopy 9
   3.4 X-ray Diffraction 12

4. CONCLUSIONS 15
   4.1 Selected Observations from Sample Analysis 15
      4.1.1 Comparison of Replicate Samples 15
      4.1.2 XRD Patterns 17
   4.2 Path Forward 18

5. REFERENCES 18

APPENDIX A Sample Cross sections 21

APPENDIX B XRD Patterns 35

FIGURES

Figure 1. Comparison of small- and large-format capsules. 5
Figure 2. Original capsule lid design. 5
Figure 3. Modified capsule lid design. 6
Figure 4. Cross section of sample 1. 8
Figure 5. Cross sections of samples 5, 10, and 15 (pressed at 700, 900, and 1100°C, respectively). 8
Figure 6. Cross sections of samples 18 and 19. 9
Figure 7. Cross section of sample 2 (100× magnification). 10
Figure 8. Cross section of sample 9 (100× magnification). 10
Figure 9. Cross section of sample 26 (100× magnification). 11
Figure 10. Cross section of sample 5 (100× magnification). 11
Figure 11. Cross section of sample 6 (100× magnification). 12
Figure 12. XRD patterns obtained from samples 12, 13, 14, and 16. 13
Figure 13. XRD patterns obtained from samples 26–28. 14
Figure 14. XRD patterns obtained from samples 18 and 19. 15
Figure 15. Cross sections of samples 2, 3, and 4 (left to right). 16
Figure 16. Cross sections of samples 7, 8, and 9 (left to right). 16
Figure 17. Cross sections of samples 12, 13, and 14 (left to right). 16
Figure 18. Cross sections of samples 22 and 23 (left to right). 17
Figure 19. Cross sections of samples 26, 27, and 28 (left to right). 17

Figure A1. Cross section of sample 1. 21
Figure A2. Cross section of sample 2. 21
Figure A3. Cross section of sample 3. 22
Figure A4. Cross section of sample 4. 22
Figure A5. Cross section of sample 5. 23
Figure A6. Cross section of sample 6. 23
Figure A7. Cross section of sample 7. 24
Figure A8. Cross section of sample 8. 24
Figure A9. Cross section of sample 9. 25
Figure A10. Cross section of sample 10. 25
Figure A11. Cross section of sample 11. 26
Figure A12. Cross section of sample 12. 26
Figure A13. Cross section of sample 13. 27

Figure A14. Cross section of sample 14. 27
Figure A15. Cross section of sample 15. 28
Figure A16. Cross section of sample 16. 28
Figure A17. Cross section of sample 17. 29
Figure A18. Cross section of sample 18. 29
Figure A19. Cross section of sample 19. 30
Figure A20. Cross section of sample 20. 30
Figure A21. Cross section of sample 21. 31
Figure A22. Cross section of sample 22. 31
Figure A23. Cross section of sample 23. 32
Figure A24. Cross section of sample 26 (large format). 32
Figure A25. Cross section of sample 27 (large format). 33
Figure A26. Cross section of sample 28 (large format). 34

Figure B1. XRD patterns collected from samples 1–4. 36
Figure B2. XRD patterns collected from samples 5, 6, 11, and 15. 37
Figure B3. XRD patterns collected from samples 7–9. 38
Figure B4. XRD patterns collected from samples 10 and 17. 39
Figure B5. XRD patterns collected from samples 12–16. 40
Figure B6. XRD patterns collected from samples 18 and 19. 41
Figure B7. XRD patterns collected from samples 20–23. 42
Figure B8. XRD patterns collected from samples 26–28. 43

TABLES

Table 1. Sample description and pressing conditions 3
Table 2. Sample density 7

ACRONYMS

AgA	silver-exchanged zeolite type A
AgX	silver-exchanged faujasite
AgZ	silver-exchanged mordenite
FCC	face-centered cubic
HIP	hot isostatic pressing
I-AgX	iodine-loaded silver-exchanged faujasite
I-AgZ	iodine-loaded silver-exchanged mordenite
ORNL	Oak Ridge National Laboratory
XRD	X-ray diffraction

HOT ISOSTATIC PRESSING OF ENGINEERED FORMS OF I-AgZ

1. INTRODUCTION

Hot isostatic pressing (HIP) is being considered as a process that could directly convert ^{129}I-bearing materials to a durable radiological waste form. The removal of volatile radioactive ^{129}I from the off-gas of a nuclear fuel reprocessing facility will be necessary to comply with regulatory requirements regarding reprocessing facilities sited within the United States, and any iodine-containing media or solid sorbents generated by off-gas abatement processes will require disposal (Jubin et al. 2012). Zeolite minerals, specifically silver-exchanged mordenite (AgZ), have been studied extensively as potential radioactive iodine sorbents and will contain ^{129}I as chemisorbed AgI, a relatively insoluble mineral with a high melting point. Oak Ridge National Laboratory (ORNL) has conducted several recent studies on the HIP of both I-AgZ and other iodine-bearing zeolite minerals.

The goal of these research efforts is to achieve a stable, highly leach resistant material that is reduced in volume as compared to bulk iodine-loaded I-AgZ. Through the use of HIP, it may be possible to achieve this with the addition of little or no additional materials (waste formers). Other goals for the process include that the waste form will be tolerant to high temperatures and pressures, not chemically hazardous, and that the process will result in in the production of less secondary waste than many of the alternative approaches currently being proposed. Early scoping studies investigated the effects of selected pressing conditions on six samples of AgZ in an engineered pellet form and two samples of chemisorbed I-AgZ and found that HIP of AgZ resulted in a waste form 2.7–3.4× more dense than the starting material (Jubin et al. 2014).

Following these initial studies, a more comprehensive research effort was designed to explore HIP of pure sodium mordenite, pure AgZ, and engineered AgZ. These materials were mixed with a known amount of iodine as either NaI or AgI and pressed using a range of temperatures and pressures. Analysis of the pressed samples indicated that the bulk phase converted to quartz (SiO_2) with AgI inclusions (Bruffey and Jubin 2015). It was unknown whether these inclusions were distinctive to the pressing process or whether they were an artifact of sample preparation and AgI incorporation into the zeolite by bulk mixing.

The most recent work completed at ORNL investigated both the outstanding question of AgI inclusions and the potential for formation of iodosodalite by HIP using varied source materials (Bruffey et al. 2017a). Studies showing the conversion of iodine-bearing zeolite minerals to iodosodalite have been conducted, but this conversion has not been demonstrated for I-AgZ (Sheppard et al. 2006; Maddrell 2005). Conversion to iodosodalite, a well-characterized mineral, is desirable as it could substantially decrease the amount of research required to assess its long-term stability, as compared with other less-understood potential iodine waste forms. To this end, a sample set was designed with three base materials: pure AgZ, pure silver-exchanged faujasite (AgX), and pure silver-exchanged zeolite type A (AgA). Iodine was incorporated into the materials by either chemisorption from a dry gas stream or occlusion, in which AgI was incorporated by grinding into a fine powder and heating at 400°C to encourage migration of iodine into the zeolite cage structure.

Analysis of the pressed samples showed that all samples using AgA as the source material converted to an iodosodalite. AgX samples in which iodine was incorporated via occlusion also converted to iodosodalite. Some samples containing sodalite also had additional mineral phases present, including AgI and nepheline, a 1:1 aluminosilicate. No samples using AgZ as the base material converted to iodosodalite. The method of iodine incorporation was shown to have an impact. AgX samples in which iodine was incorporated by chemisorption were not observed to convert to sodalite, differing from the iodine-loaded AgX samples prepared by occlusion.

1.1 Waste Form Performance Testing

There is a significant outstanding question regarding the conversion by HIP of I-AgZ to a radioactive waste form. A key component of any radioactive waste form is its ability to retain the target radionuclide for an extended time. Durability testing for homogenous waste forms, such as glass, have been developed and standardized to measure the corrosion of the waste form and retention of the target radionuclides under potential geologic repository conditions. However, the waste forms produced by HIP of I-AgZ are heterogenous and appear to contain AgI encapsulated by a quartz or mineral matrix. It is unclear how common waste form performance test methods translate to heterogeneous or encapsulated mineral waste forms. Limited performance testing using product consistency test methods was completed on several of the waste forms generated through previous efforts, and approximately half of the tested samples showed no measurable iodine release (Bruffey and Jubin 2016).

Active research efforts focus on the development of new performance testing methods for AgI-containing heterogenous waste forms (Ebert et al. 2016). These methods are under development at Pacific Northwest National Laboratory and at Argonne National Laboratory, and collaborative test development efforts between these laboratories and ORNL are ongoing. These methods are intended to account for both chemical dissolution of AgI at exposed waste form surfaces and within grain boundaries of the waste form interior. Given that the chemical dissolution rate of AgI is slow and that the total solubility of AgI is very slow (pK_{sp} = 16 at 25°C), an effort to accelerate dissolution will be conducted using electrochemical dissolution methods.

1.2 Objectives and Sample Set

The samples detailed in this report are intended to support ongoing development of iodine waste forms by generating a suite of HIPed I-AgZ samples. These samples are distinct from previous efforts in that they are prepared exclusively with an engineered form of AgZ manufactured using a binder. Iodine was incorporated solely by chemisorption. This base material is expected to be more representative of an operational system than were samples prepared previously with pure minerals.

The 27 samples listed in Table 1 can be tested for waste form durability and radionuclide retention upon the successful deployment of currently evolving durability test methods. The results of this durability testing could be used to investigate several outstanding questions. First, the inherent variability in measured properties for identical waste forms produced by HIP of I-AgZ is unknown. To better understand this variability, four sets of small-format replicate samples were included in the test matrix. These are samples 2–4, 7–9, 12–14, and 22–24. Each set of replicate samples was manufactured using the same batch of source material and the same capsule loading and sealing procedures, and was pressed under the same conditions in a single batch.

Table 1. Sample description and pressing conditions

Sample	Temp. (°C)	Pressure (MPa)	Time (h)	Drying temp. (°C)	Notes
1	700	100	3	–	
2	700	175	3	–	
3	700	175	3	–	
4	700	175	3	–	
5	700	300	3	–	
6	900	100	3	–	
7	900	175	3	–	
8	900	175	3	–	
9	900	175	3	–	
10	900	300	3	–	
11	1100	100	3	–	
12	1100	175	3	–	
13	1100	175	3	–	
14	1100	175	3	–	
15	1100	300	3	–	
16	900	175	6	–	
17	900	175	12	–	
18	525	100	3	–	
19	525	100	12	–	
20	900	175	3	150	
21	900	175	3	270	
22	900	175	3	450	
23	900	175	3	450	
24	900	175	3	450	Failed capsule
26	900	175	3	–	Scaled-up sample
27	900	175	3	–	Scaled-up sample
28	900	175	3	–	Scaled-up sample
Note: The preparation of Sample 25 was reported in Bruffey, et al. (2017b) as part of a concurrent research effort. The sample consisted of pure AgI powder and was pressed at 900°C and 300MPa.					

Second, although there has been some limited effort to determine the effect of pressing conditions on sample properties, optimized pressing conditions including pressure, temperature, and time cannot be fully developed without the results of durability testing. This sample set will allow for systematic evaluation of how durability is affected by pressing conditions using a realistic engineered source material (i.e., I-AgZ). The sample set described in Table 1 will allow evaluation of the effect of pressure (100–300 MPa), temperature (525–1100°C), and pressing time (3–12 h) with all other variables held constant.

Third, the effect of water on the HIP process is not well understood. Previous work observed significant void space and cracking on the surface of the sample cross section, and it has been proposed that this could

result from physisorbed water on the source minerals. In this effort, three samples were loaded with iodine and then dried at selected temperatures (150–450°C) to determine if a drying step could decrease the amount of void space present in the pressed samples.

Finally, although HIP is a well-known industrial process commonly performed at large scale, previous work on I-AgZ waste forms has been limited to small-format samples. This work prepared three samples that were 2× the diameter and height of the small-format capsules used thus far, i.e. 8 × the total sample volume. These samples are a scoping test to evaluate whether scaled-up HIP of I-AgZ presents any direct concerns. The three large-format samples were pressed in triplicate with a single set of HIP conditions.

This sample set will be stored at ORNL and made available for collaborators working on development of performance test methods. The questions raised in this section cannot be fully answered without an understanding of how pressing conditions and sample preparation affect the long-term durability and iodine retention of the waste form. Given that these waste form durability test methods are still under development, this document details the preparation of the sample set and serves as a repository of the preliminary characterization efforts for these samples. The densities, mineral phases, and visual appearances of each sample are discussed within the body of the report, and full datasets are provided in the appendices. It is important that this data and the prepared samples be available and easily referenced in complement of future waste form durability testing.

2. MATERIALS AND METHODS

2.1 Preparation of I-AgZ

All samples used engineered, pelletized silver mordenite (Zeolon 900) from Molecular Products (Ionex-Type Ag 900 E16) as the source material. It contained 9.5% silver by weight and has 1/16 in. pellet diameter. The material was hydrogen reduced at 270°C prior to iodine loading.

AgZ was loaded with iodine by contacting the material with a 50 ppmv I_2 stream (balance dry air) at a gas velocity of 10 m/min. AgZ was contained within a tube furnace at 150°C during iodine loading. The iodine concentration of the effluent stream was monitored periodically by diversion through a 1*M* NaOH scrubber. The iodine concentration in the scrubber was analyzed by ion-selective electrode. Iodine loading was considered complete after the effluent iodine concentration remained constant for 24 h. The loaded material was then purged with dry air for 24 h to remove physisorbed iodine. The final iodine content of the material was determined to be 87.8 mg/g AgZ by neutron activation analysis conducted at ORNL's High Flux Isotope Reactor.

Samples 20–24 underwent an additional drying step after iodine loading. For each temperature (150, 270, and 450°C), AgZ was dried in a tube furnace (1.87 in. diameter) for 24 h under a low flow of argon. The flow rate was set such that the superficial gas velocity was equivalent to 1.46 m/min at all three temperatures. After removal from the tube furnace, samples 20–24 were blanketed with argon until capsule sealing.

2.2 Encapsulation, Pressing, and Mounting

As was mentioned previously, two capsule sizes were used. Small-format samples were fabricated from tubing with an outer diameter of 3/4 in. Each small-format capsule was 1 in. in length. Large-format samples were doubled in diameter (1.5 in.) and length (2 in.), preserving the length-to-diameter ratio of the small-format capsules. The sample capsules were constructed of 304 stainless steel tubing. The wall thickness of the tubing and the end cap was 0.020 in. The two capsules are shown in Figure 1.

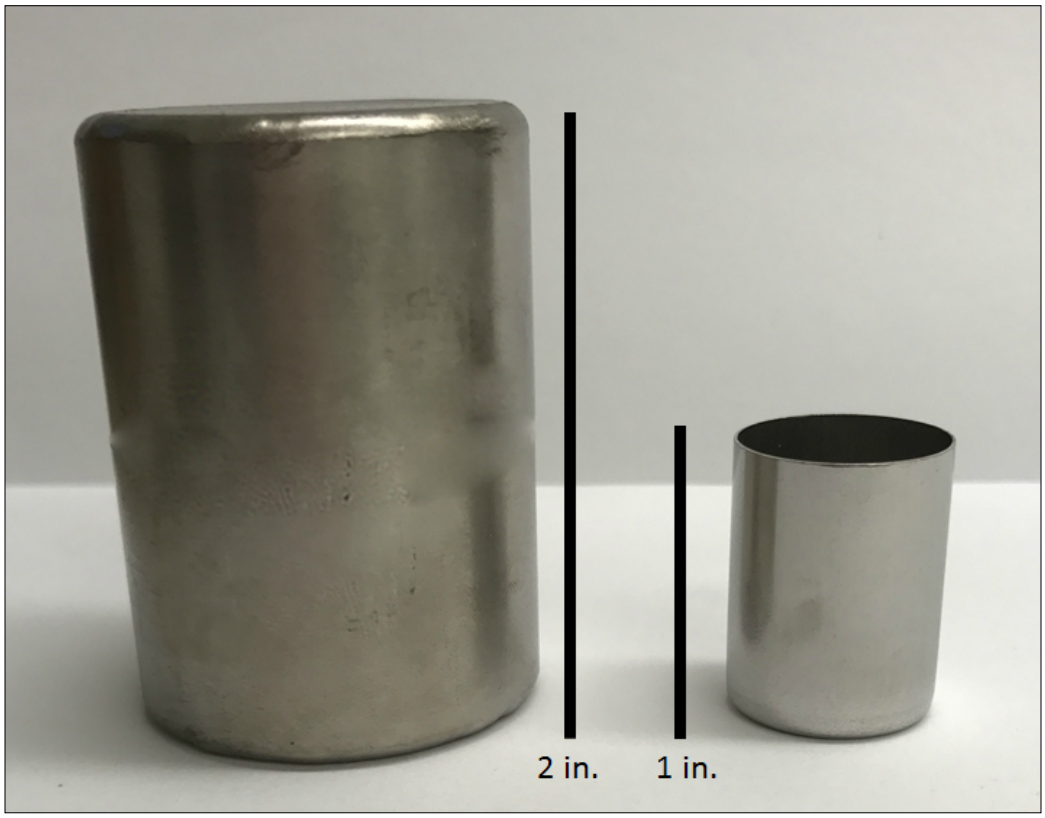

Figure 1. Comparison of small- and large-format capsules.

Figure 2. Original capsule lid design.

Figure 3. Modified capsule lid design.

Previous work at ORNL has resulted in substantial improvements to capsule design and sealing. The original capsule design (Figure 2) was a right cylindrical cylinder with a flat metal lid welded onto the top after sample emplacement. Refinements to the capsule lid design are described in Bruffey and Jubin (2015). The lid used in this effort, for both large- and small-format samples, was an inset trepan lid with a vent port (Figure 3).

The sample capsules were loaded by pouring I-AgZ into the capsules and shaking lightly to ensure even packing. There was a gap of 1/8 in. in length between the material and the capsule lid. The total amount of material used in each small-format sample was ~5 g. Large-format samples contained ~45 g.

Samples 20–24, which underwent additional drying after iodine loading, were transferred directly from an argon-blanketed vial to a vacuum box for attachment of the capsule lid and closure of the vent port by electron beam welding. The lids of the remaining samples were welded onto the capsules on a benchtop and transferred to a vacuum box only for closure of the vent port by electron beam welding.

After each sample had been sealed it was hydrostatically leak-checked. The samples were placed in a bell jar and pressurized to 1450 psi. An increase in weight of the capsule after pressurization indicated in-leakage of water. Sample 24 was found to leak and was discarded.

The samples were processed using HIP by American Isostatic Presses, Inc., according to the conditions provided in Table 1 and then returned to ORNL. Sample 27 did not compress successfully, which resulted in an artificially low density and failure to form a monolithic body within the capsule. This failure likely resulted from a small leak that was not detected by hydrostatic leak testing.

3. ANALYSIS

3.1 Density of Pressed Samples

After HIP, the density of each sample was determined in triplicate by pycnometer using isopropyl alcohol as the fill liquid. The measured density was adjusted to remove the contribution of the stainless steel capsule and assumes that the density of the stainless steel capsule material is not altered by HIP. The adjusted density of each I-AgZ sample is shown in Table 2. (The reported error represents one standard deviation.)

Table 2. Sample density

Sample	Temp. (°C)	Pressure (MPa)	Time (h)	Drying temp. (°C)	Density	
					(g/mL)	+/-
1	700	100	3	–	2.649	0.0165
2	700	175	3	–	2.671	0.007
3	700	175	3	–	2.642	0.0325
4	700	175	3	–	2.683	0.0075
5	700	300	3	–	2.161	0.005
6	900	100	3	–	2.645	0.0065
7	900	175	3	–	2.742	0.0315
8	900	175	3	–	2.735	0.0105
9	900	175	3	–	2.730	0.065
10	900	300	3	–	2.749	0.0165
11	1100	100	3	–	2.548	0.0185
12	1100	175	3	–	2.689	0.014
13	1100	175	3	–	2.718	0.0825
14	1100	175	3	–	2.746	0.08
15	1100	300	3	–	2.674	0.0065
16	900	175	6	–	2.715	0.021
17	900	175	12	–	2.643	0.068
18	525	100	3	–	1.701	0.005
19	525	100	12	–	1.718	0.018
20	900	175	3	150	2.666	0.0145
21	900	175	3	270	2.760	0.0105
22	900	175	3	450	2.751	0.0335
23	900	175	3	450	2.765	0.031
26 (scaled-up)	900	175	3	–	2.657	0.1455
27 (scaled-up)	900	175	3	–	1.364[a]	0.0505
28 (scaled-up)	900	175	3	–	2.711	0.2

[a]Sample did not compress.
Grey shading indicates replicate samples.

3.2 Visual Examination

Following density measurements, all capsules were cross sectioned, and one half was mounted in epoxy and polished to facilitate further analysis. The outer diameter of the epoxy and plastic dish used for mounting of the small-format and large-format samples was 30.2 and 49.2 mm, respectively.

The cross section of each sample is shown in Appendix A, and several are shown here to illustrate common sample features. The sample surface is typically brown or dark brown (Figure 4). Some samples display a light green edge at the capsule wall, and this edge is more prominent at higher temperatures (Figure 5). Visually, some pellet structure appears to be retained at all temperatures. Pressure variations do not result in a visual difference between samples.

Figure 4. Cross section of sample 1.

Figure 5. Cross sections of samples 5, 10, and 15 (pressed at 700, 900, and 1100°C, respectively).

Samples 18 and 19, which were pressed at 525°C, have surfaces that are noticeably more heterogenous than the others (Figure 6).

Figure 6. Cross sections of samples 18 and 19.

Previous efforts have noted the presence of voids and cracks in many of the pressed samples. These features were not observed to the same extent in this effort.

3.3 Optical Microscopy

All samples were examined by optical microscopy at 100× magnification. Selected samples are shown here. Samples 2, 6, and 26 (Figures 7–9) show representative sample surfaces. In general, the samples are brown and flecked throughout with black and light-colored inclusions. There are typically some larger-scale features or inclusions that are darker brown in color. This is illustrated in Figure 7. As mentioned previously, there are often edge layers adjacent to the capsule wall that are lighter in color (Figure 8). The large-format samples that were successfully pressed demonstrate similar features to the small-format samples (Figure 9).

Optical microscopy does allow for better examination of small hairline cracks that are present in some samples (Figures 9 and 10). These cracks vary in width and depth. Figures 10 and 11 show that, in some cases, there is a gap between the pressed I-AgZ and the capsule wall.

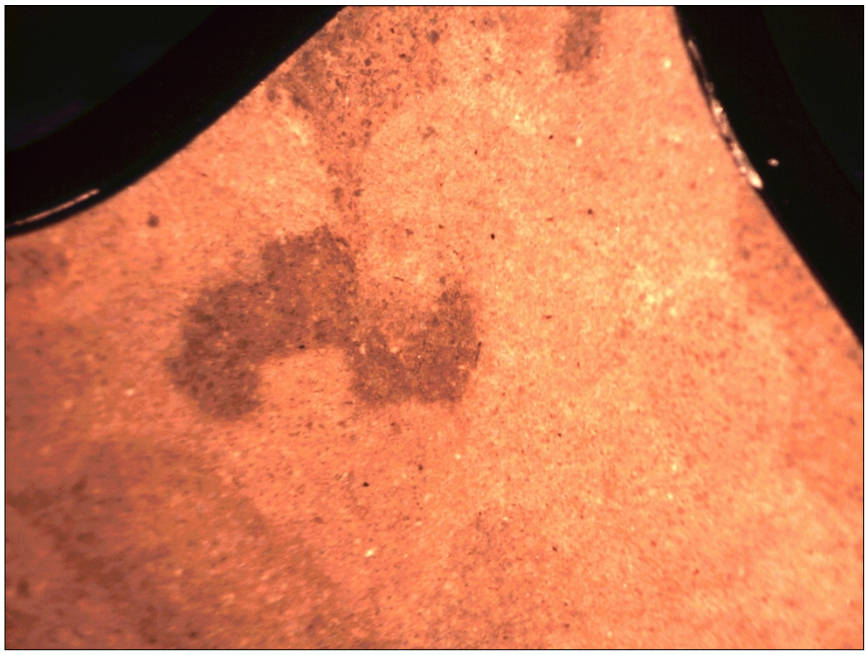

Figure 7. Cross section of sample 2 (100× magnification).

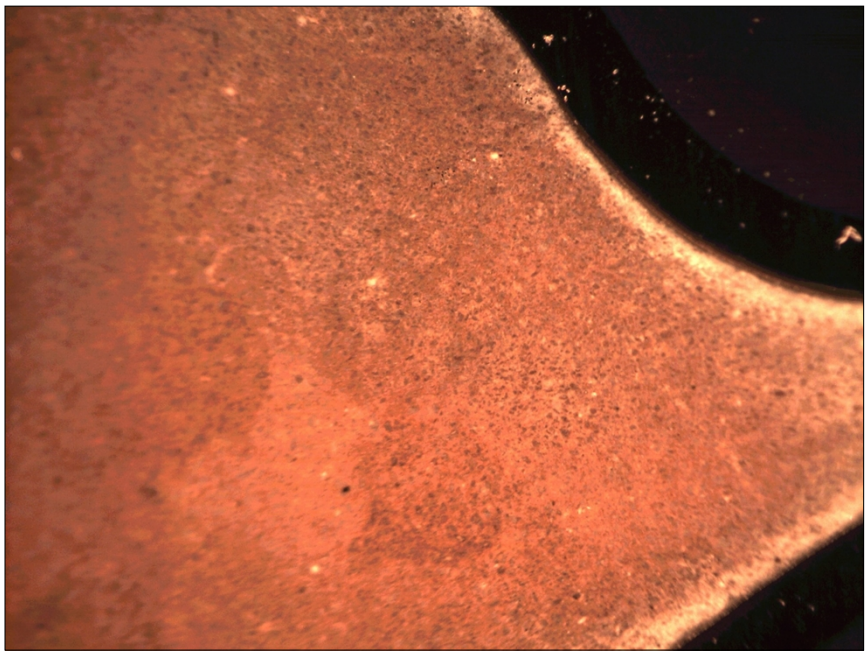

Figure 8. Cross section of sample 9 (100× magnification).

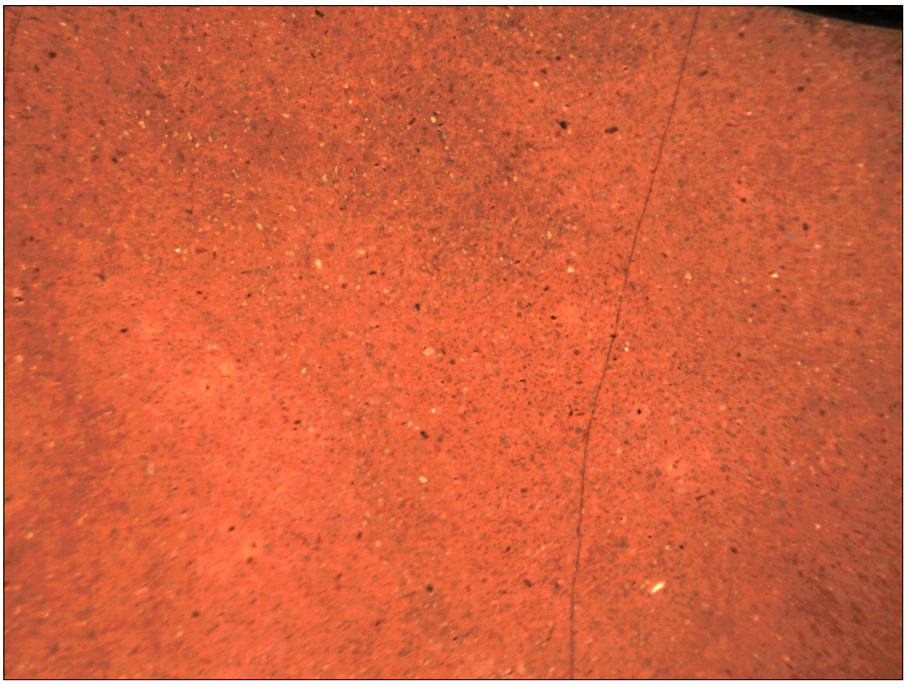

Figure 9. Cross section of sample 26 (100× magnification).

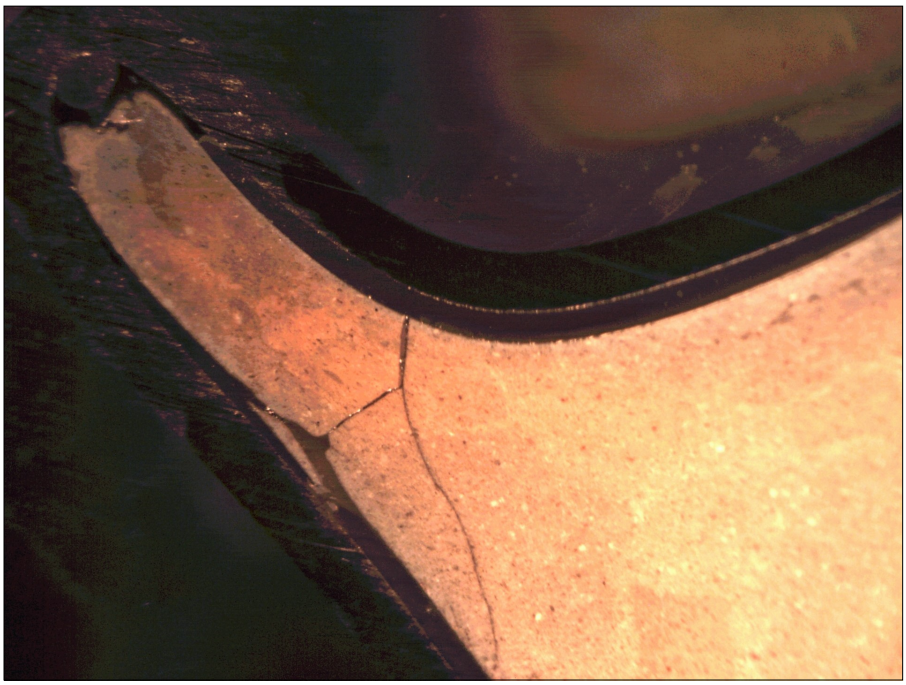

Figure 10. Cross section of sample 5 (100× magnification).

Figure 11. Cross section of sample 6 (100× magnification).

3.4 X-ray Diffraction

Continuous θ-2θ scans were performed on the Panalytical X'pert diffractometer from nominally 5° to 70° or 90° 2θ using CuKα radiation (λ = 1.540598 Å) and the X'Celerator detector. All scans used 0.25° fixed slits, 0.50° antiscatter slit, and 0.04° Soller slits coupled with a 10 mm mask (beam width). A nickel filter was used to remove the CuKβ peaks. For the phase identification procedure, a search match was conducted using Jade software (2012) with the ICDD database (2013). The x-ray diffraction (XRD) patterns for all samples are shown in Appendix B, and selected patterns are discussed here.

All but two samples exhibited five mineral phases in addition to the FeNi alloy of the stainless steel capsule. The identified phases included (1) triclinic SiO_2, (2) face-centered cubic (FCC) silver, (3) FCC FeNi alloy, (4) AgI (iodargyrite), (5) $Mg_2Al_4Si_5O_{18}$ (indialite), and (6) mordenite [with a nominal composition of $K_{1.5}NaCaAl_{4.5}Si_{19.5}O_{48}(H_2O)_{14.5}$]. A representative pattern for samples showing these six phases is shown in Figure 12 using the patterns collected for samples 12, 13, 14, and 16. Peaks are marked to represent correspondence to triclinic SiO_2 (1), AgI (4), indialite (5), and mordenite (6). The dotted lines are the observed peaks of the mordenite phase.

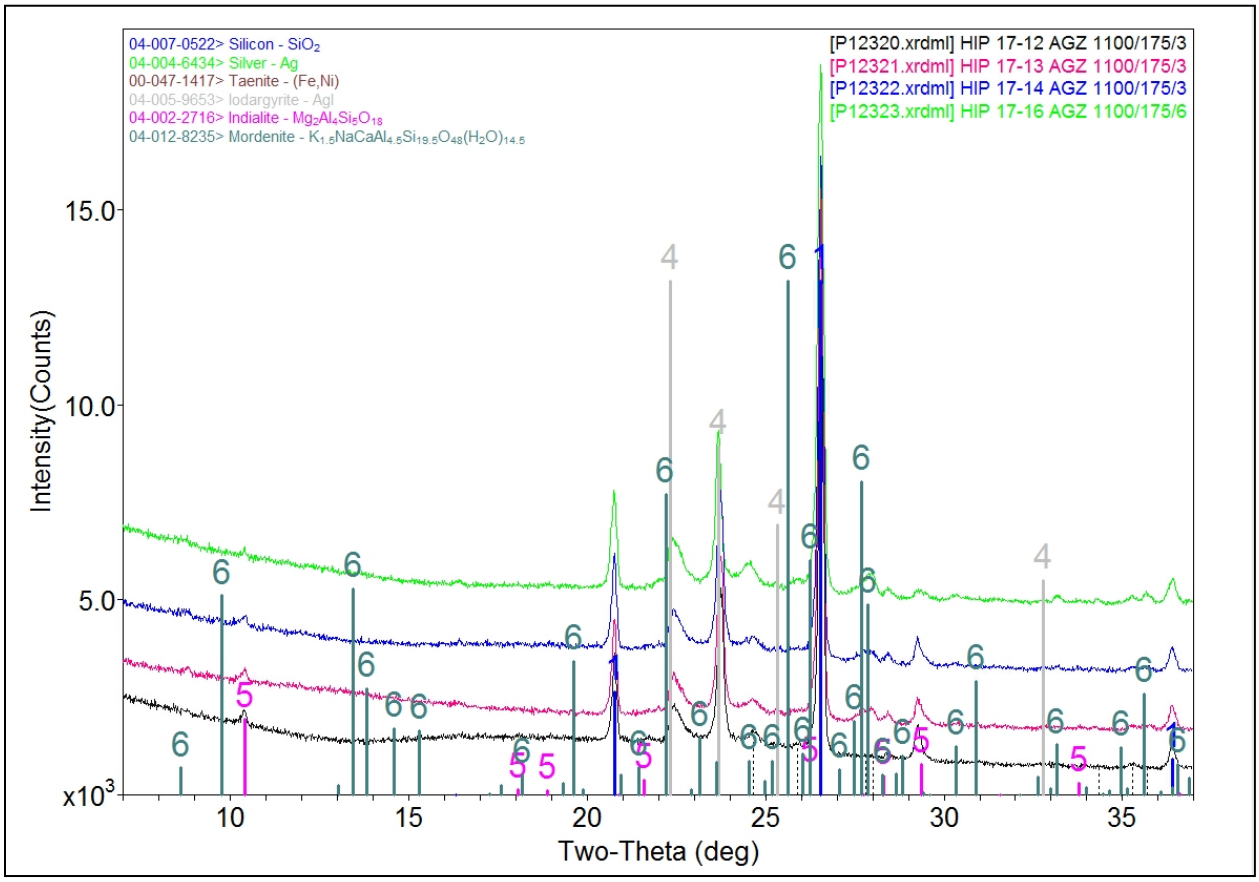

Figure 12. XRD patterns obtained from samples 12, 13, 14, and 16.

The patterns of the three large-format samples (26–28) are shown in Figure 13. The patterns collected for these samples were not distinct from the representative pattern shown in Figure 12 and show the same six identified phases [triclinic SiO_2 (1), FCC silver (2), FCC FeNi alloy (3), AgI (4), indialite (5), and mordenite (6)].

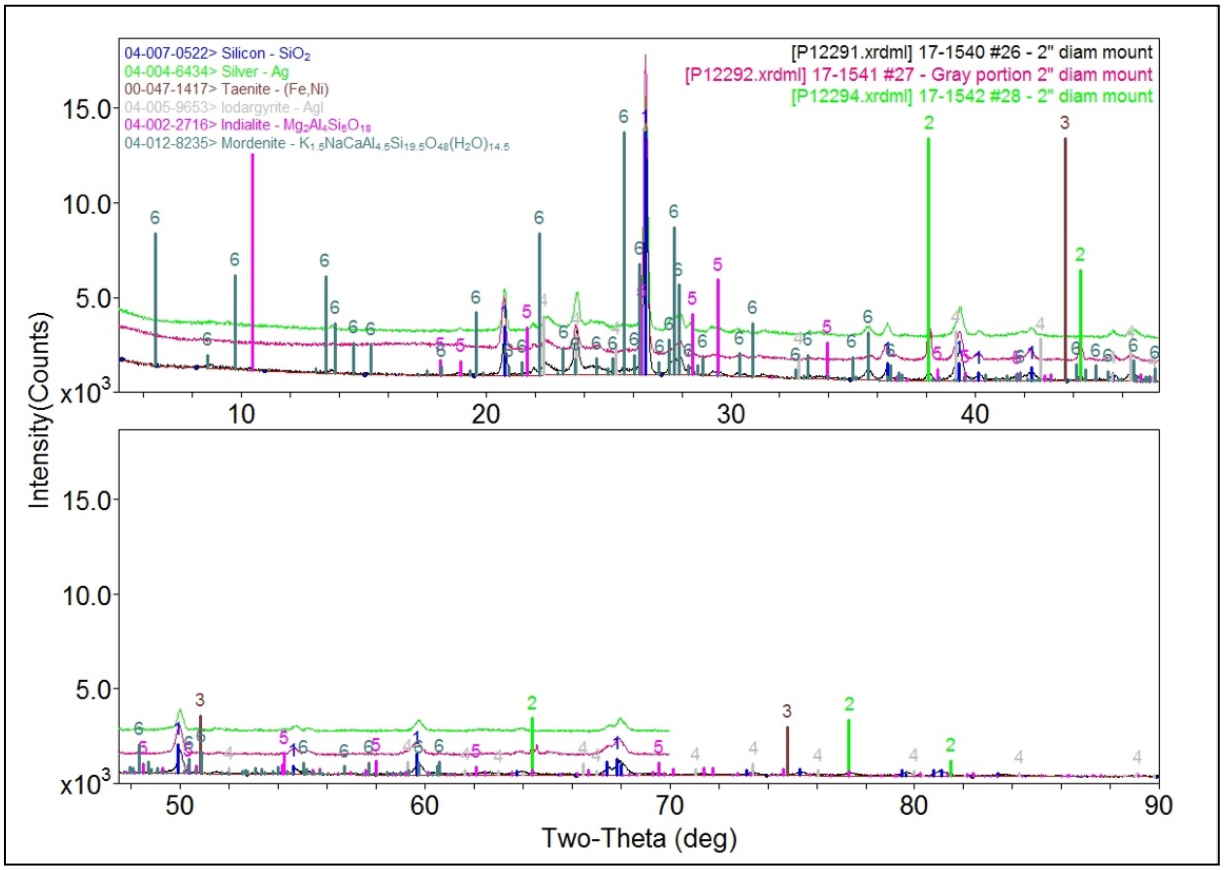

Figure 13. XRD patterns obtained from samples 26–28.

Samples 18 and 19 were the only samples that demonstrated an XRD pattern substantially different from that shown in Figure 12. These samples were pressed at the lowest temperature of the range examined (525°C), and no indialite was identified in these samples. The patterns collected from samples 18 and 19 (Figure 14) show that the mineral phases identified included triclinic SiO_2 (1), FCC silver (2), AgI (4), and mordenite (6). Note, the dotted line may be from (3) FCC FeNi alloy (from the HIP casing)

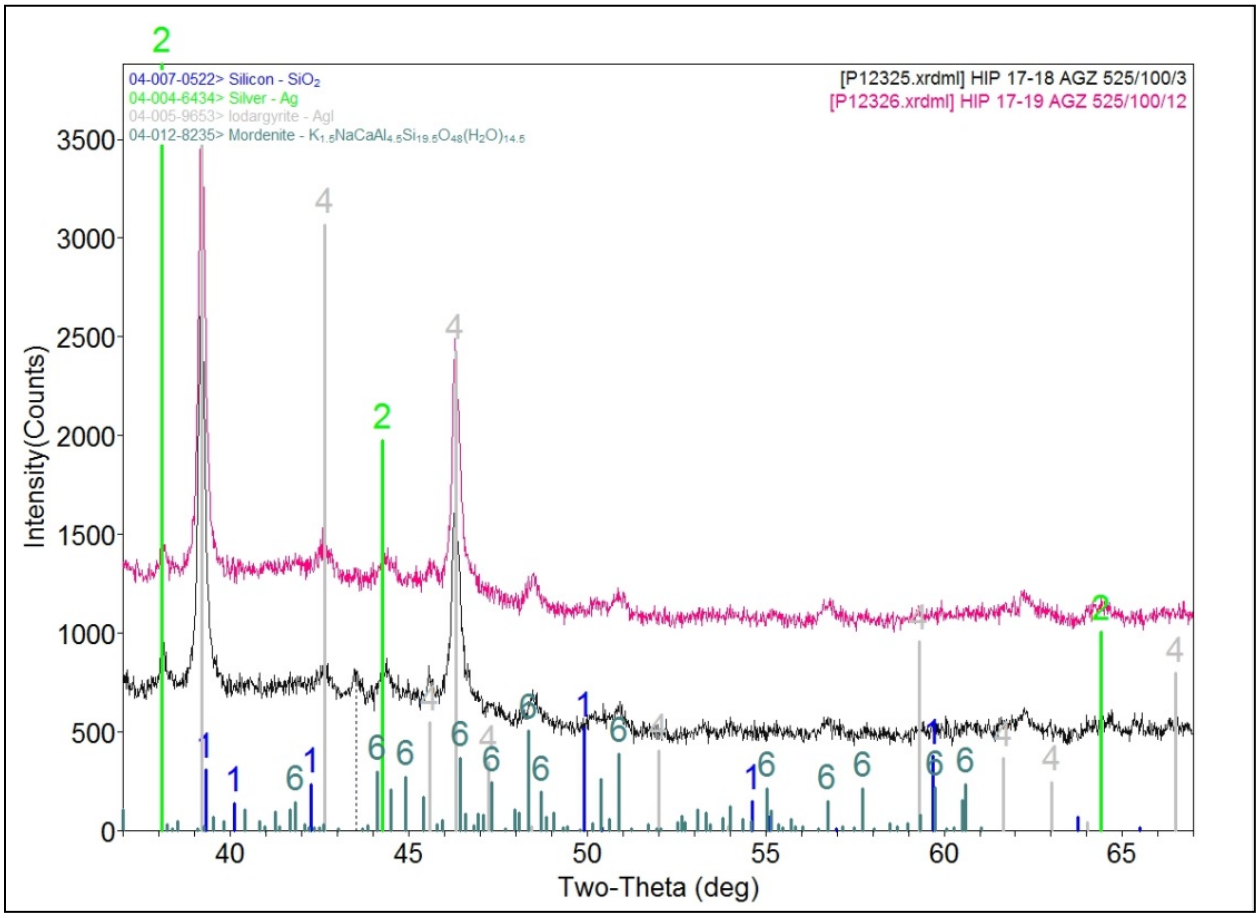

Figure 14. XRD patterns obtained from samples 18 and 19.

4. CONCLUSIONS

This report describes the preparation and initial analyses of a sample set designed to support future waste form performance testing. A few selected observations are included here, but given that the impact of the variables investigated (i.e., sample pretreatment, pressing conditions, process variability, and scaleup) cannot fully be understood without information regarding long-term durability of each sample, these observations are limited in scope.

4.1 Selected Observations from Sample Analysis

4.1.1 Comparison of Replicate Samples

Four small-format replicate sample sets and one large-format replicate sample set were included in this effort. The densities of four small-format replicate sample sets (samples 2–4, samples 7–9, samples 12–14, and samples 22–23) showed a variability of 0.01–0.1 g/mL between replicate samples. Figures 15–18 show that visually the small-format samples were very similar within each replicate set.

A capsule failure in the large-format replicate sample set resulted in only two replicate samples available for comparison. The densities of samples 26 and 28 are 2.657 ± 0.1455 g/mL and 2.711 ± 0.200 g/mL, respectively. Figure 19, which includes sample 27 (failed), shows that the surface of sample 28 has more distinguishing features than sample 26. However, no conclusions regarding the variation of the large-format samples can be drawn from such a small sample set.

Figure 15. Cross sections of samples 2, 3, and 4 (left to right).

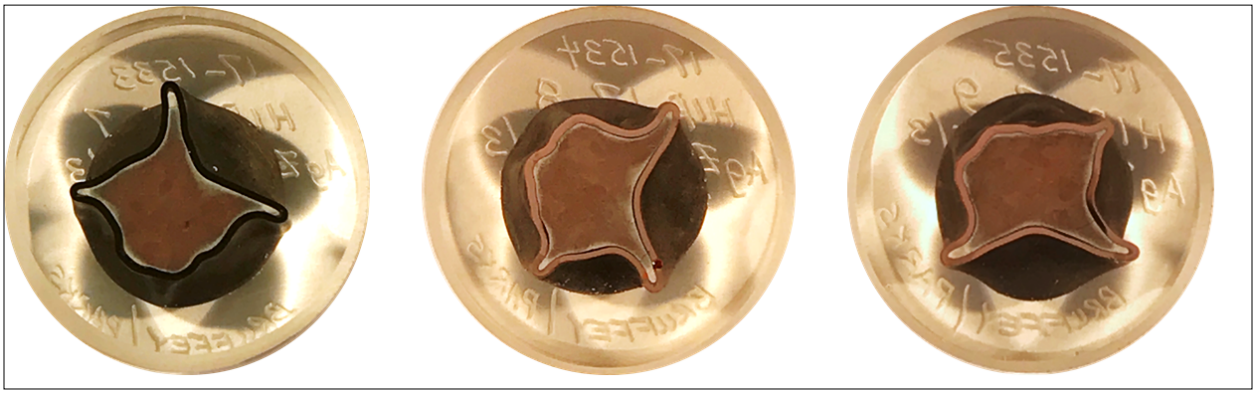

Figure 16. Cross sections of samples 7, 8, and 9 (left to right).

Figure 17. Cross sections of samples 12, 13, and 14 (left to right).

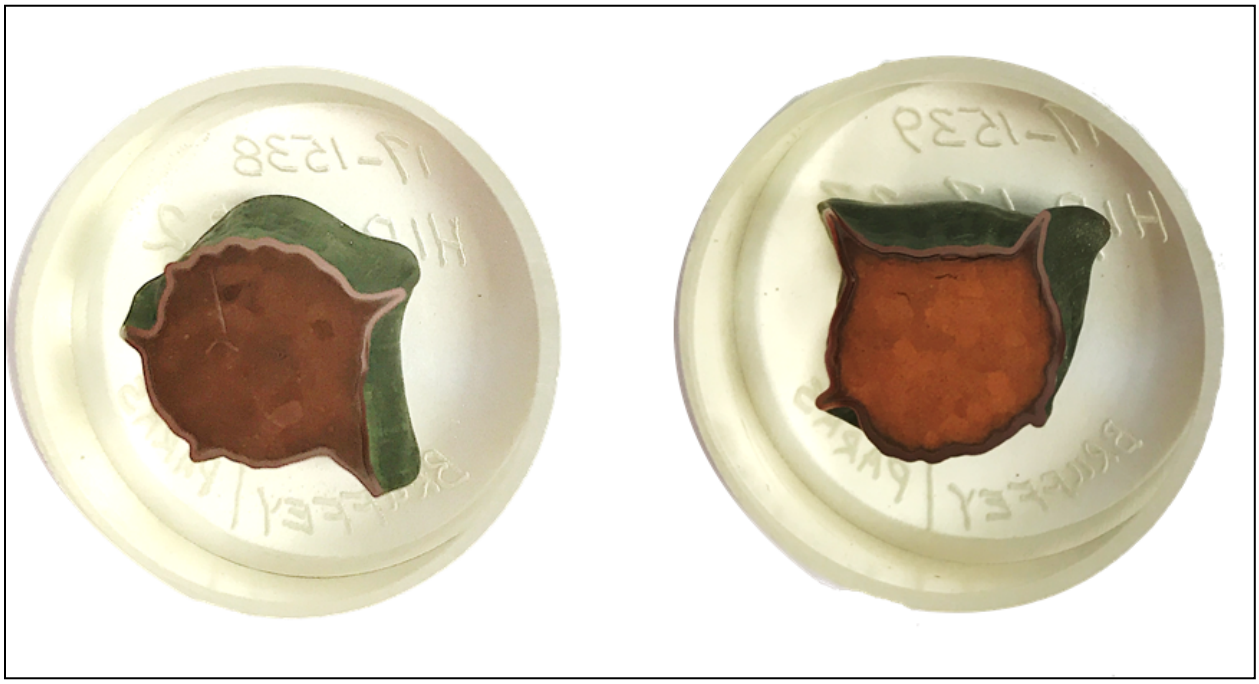

Figure 18. Cross sections of samples 22 and 23 (left to right).

Figure 19. Cross sections of samples 26, 27, and 28 (left to right).

4.1.2 XRD Patterns

The phases identified by XRD are distinct from previous efforts. First, the presence of mordenite has not previously been observed in samples pressed at ≥700°C. It was present in all samples prepared during this effort. Second, indialite, an aluminosilicate of formula $Mg_2Al_4Si_5O_{18}$, has not been observed during previous work. Several other aluminosilicate minerals have been observed, and it may be that indialite is a specific result of the binder used to manufacture the engineered form of AgZ.

Samples 18 and 19, which were pressed at 525°C, did not contain indialite but contained strong mordenite peaks. This is consistent with the previous results regarding mordenite mentioned above. Visually, samples 18 and 19 were observed to have highly heterogeneous cross sections.

4.2 Path Forward

ORNL will continue to explore the production of large-format capsules to recognize any issues that might arise during scaleup of I-AgZ waste form production by HIP. Future efforts will ensure that the capsule designs used currently are suitable for scaleup and that sample preparation and encapsulation techniques translate to a larger scale.

The sample set reported here will support waste form durability testing across the national laboratories and will provide insight into the effects of pressing conditions, sample drying, process variability, and scaleup on the produced waste form. Ultimately, optimized sample composition and pressing conditions can be determined only through waste form performance testing. ORNL will store these waste form samples until they are needed by collaborators for durability testing. Additionally, ORNL will continue to make samples from all previous efforts available as requested (Bruffey et al., 2017b).

Acknowledgments: *The authors would like to acknowledge Tom Geer for his metallurgical services and David Alan Frederick for his joining services (both of ORNL's Physical Sciences Directorate).*

5. REFERENCES

Bruffey, S. H. and R. T. Jubin. *Recommend HIP Conditions for AgZ*. Report No. ORNL/SPR-2015/503. Oak Ridge National Laboratory, Oak Ridge, TN, 2015.

Bruffey, S. H. and R. T. Jubin. "Product Consistency Testing of a Hot Isostatically Pressed Iodine-Containing Waste Form." *Transactions of the American Nuclear Society* 115 (2016): 233–235.

Bruffey, S. H., R. T. Jubin, and J. A. Jordan. *Fundamental Aspects of Zeolite Waste Form Production by Hot Isostatic Pressing*. Report No. ORNL/TM-2016/759. Oak Ridge National Laboratory, Oak Ridge, TN, 2017a.

Bruffey, S. H., J. A. Jordan, and R. T. Jubin. *Preparation of Hot Isostatically Pressed AgZ Waste Form Samples*. Report No. ORNL/TM-2017/514. Oak Ridge National Laboratory, Oak Ridge, TN, 2017b.

Ebert, W. L., T. A. Cruse, and J. L. Jerden Jr. *Testing Roadmap for Iodine Waste Forms*. Report No. FCRD-MRWFD-2016-000256. Argonne National Laboratory, Lemont, IL, 2016.

ICDD, PDF-4+ [data base]. International Centre for Diffraction Data, Newtown Square, PA, 2013.

Jade, version 9.4.5 [computer software]. Materials Data, Inc., Livermore, CA, 2012.

Jubin, R. T., N. Soelberg, D. Strachan, and G. Ilas. *Fuel Age Impacts on Gaseous Fission Product Capture During Separations*. Report No. FCRD-SWF-2012-000089, PNNL-22550, Oak Ridge National Laboratory, Oak Ridge, TN, 2012.

Jubin, R. T., S. H. Bruffey, and K. K. Patton. *Expanded Analysis of Hot Isostatically Pressed Iodine-Loaded Silver-Exchanged Mordenite*. Report No. ORNL/LTR-2014/476. Oak Ridge National Laboratory, Oak Ridge, TN, 2014.

Maddrell, E. *Capture and Immobilization of Iodine*. National Nuclear Laboratory, Sellafield, Cumbria, UK, November 2, 2005.

Sheppard, G. P., and J. A. Hriljac, E. R. Maddrell, and N. C. Hyatt. “Silver Zeolites: Iodide Occlusion and Conversion to Sodalite—A Potential I-129 Waste Form?” In *Scientific Basis for Nuclear Waste Management XXIX*, ed. P. Van Iseghem, Vol. 932. (Warrendale, PA: Materials Research Society, 2006), 775–82.

APPENDIX A

Sample Cross sections

Figure A1. Cross section of sample 1.

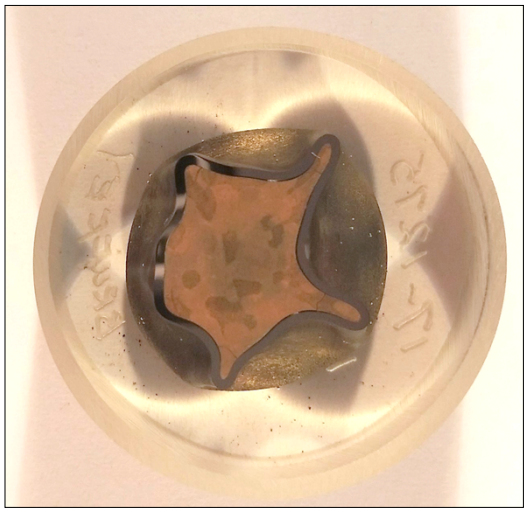

Figure A2. Cross section of sample 2.

Figure A3. Cross section of sample 3.

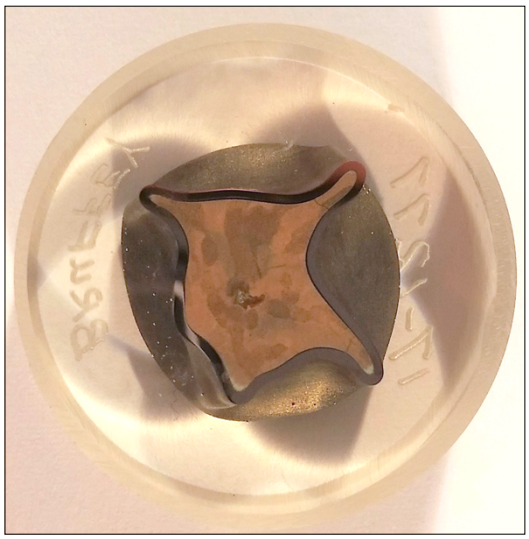

Figure A4. Cross section of sample 4.

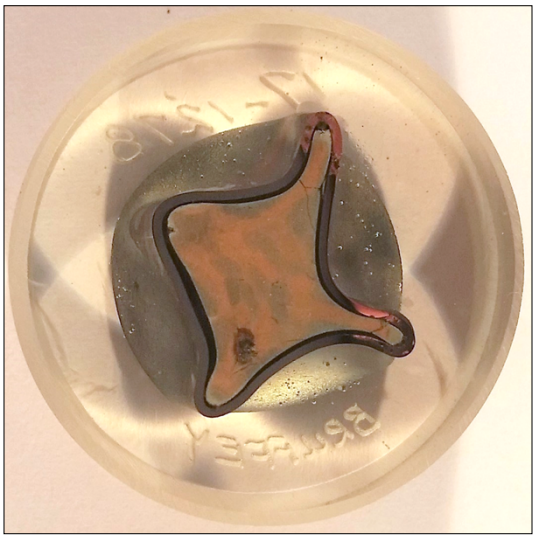

Figure A5. Cross section of sample 5.

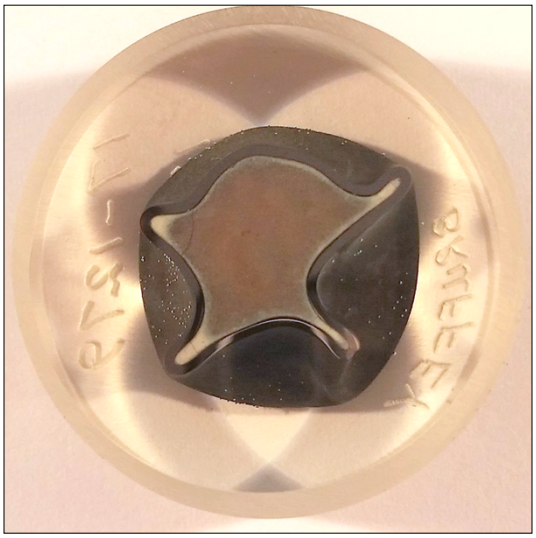

Figure A6. Cross section of sample 6.

Figure A7. Cross section of sample 7.

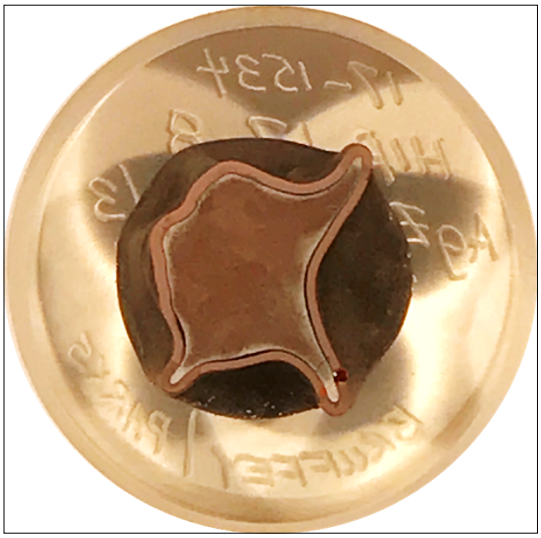

Figure A8. Cross section of sample 8.

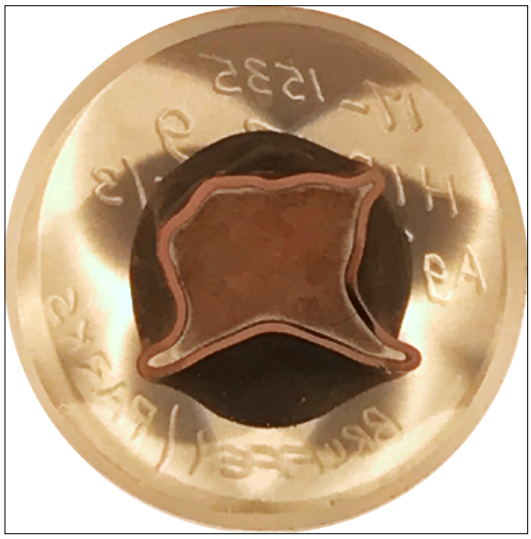

Figure A9. Cross section of sample 9.

Figure A10. Cross section of sample 10.

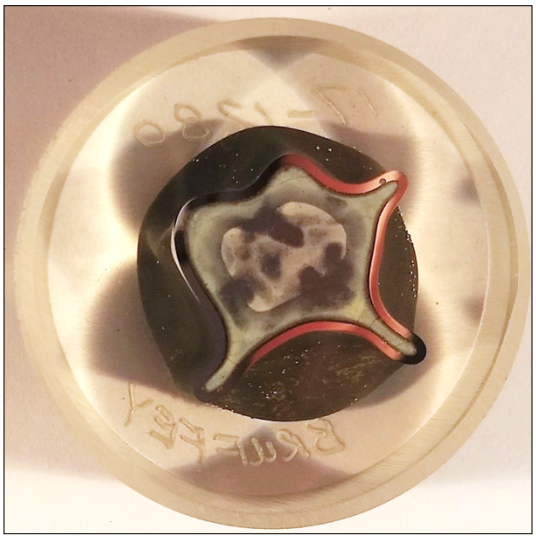

Figure A11. Cross section of sample 11.

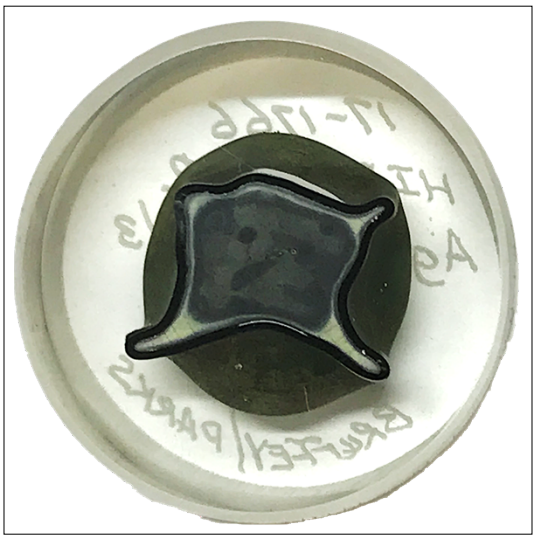

Figure A12. Cross section of sample 12.

Figure A13. Cross section of sample 13.

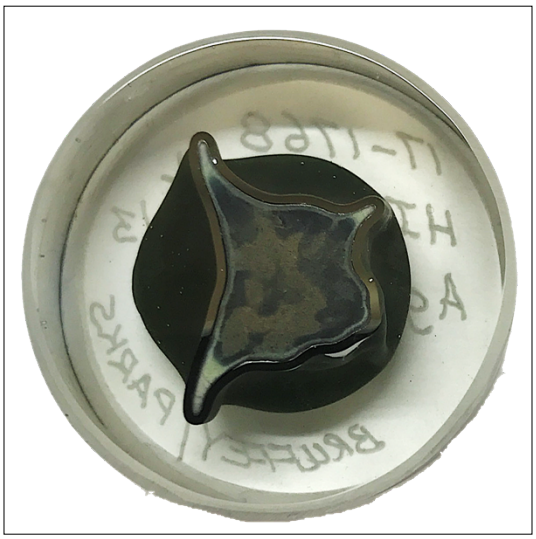

Figure A14. Cross section of sample 14.

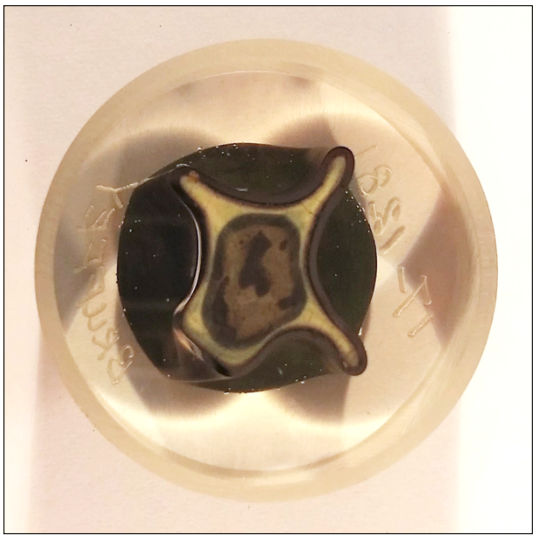

Figure A15. Cross section of sample 15.

Figure A16. Cross section of sample 16.

Figure A17. Cross section of sample 17.

Figure A18. Cross section of sample 18.

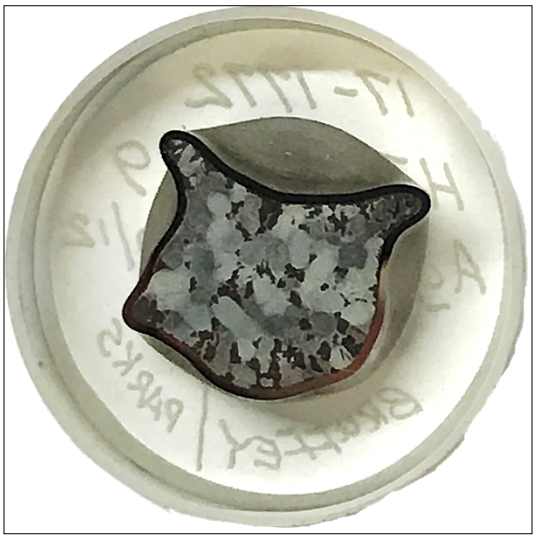

Figure A19. Cross section of sample 19.

Figure A20. Cross section of sample 20.

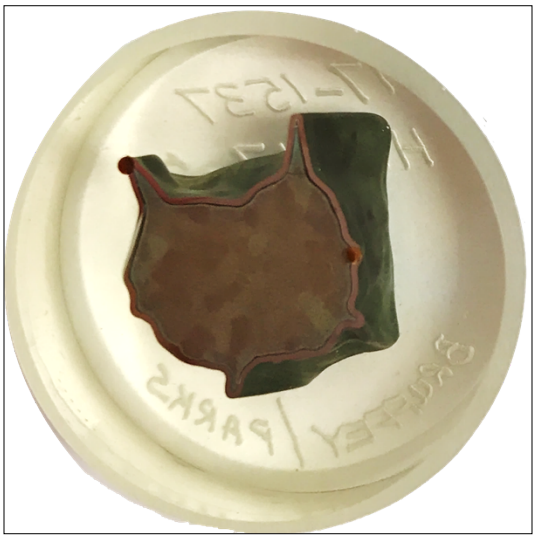

Figure A21. Cross section of sample 21.

Figure A22. Cross section of sample 22.

Figure A23. Cross section of sample 23.

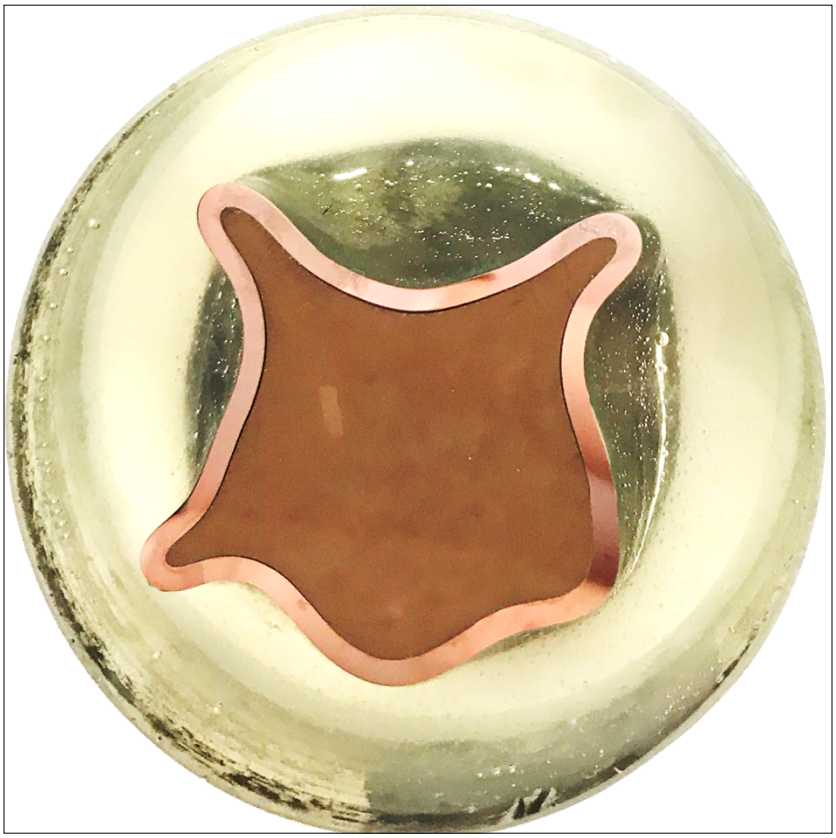

Figure A24. Cross section of sample 26 (large format).

Figure A25. Cross section of sample 27 (large format).

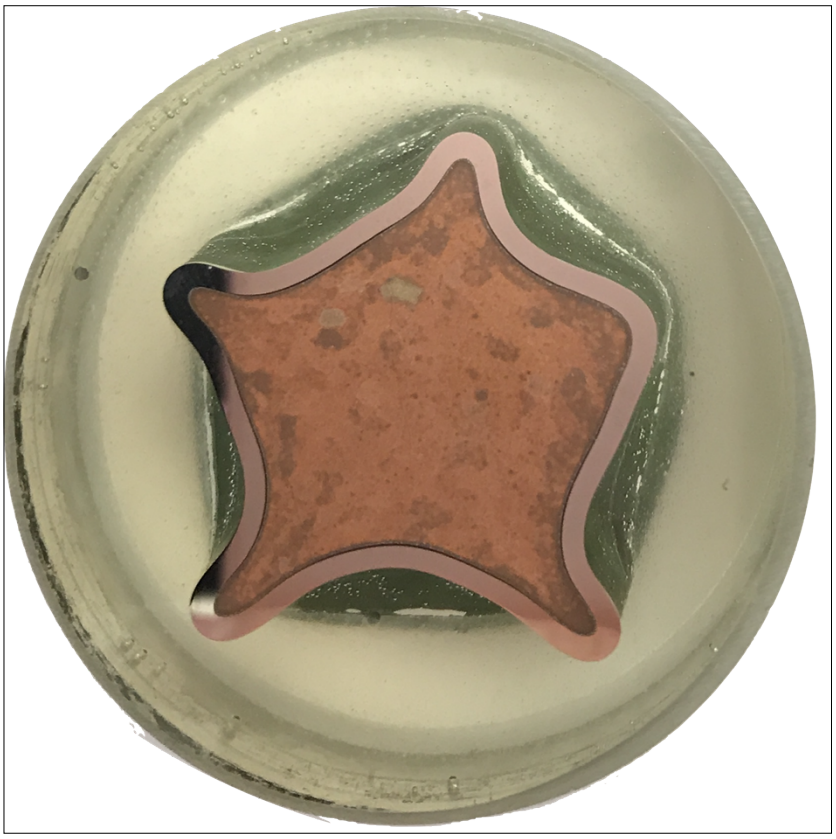

Figure A26. Cross section of sample 28 (large format).

APPENDIX B

XRD Patterns

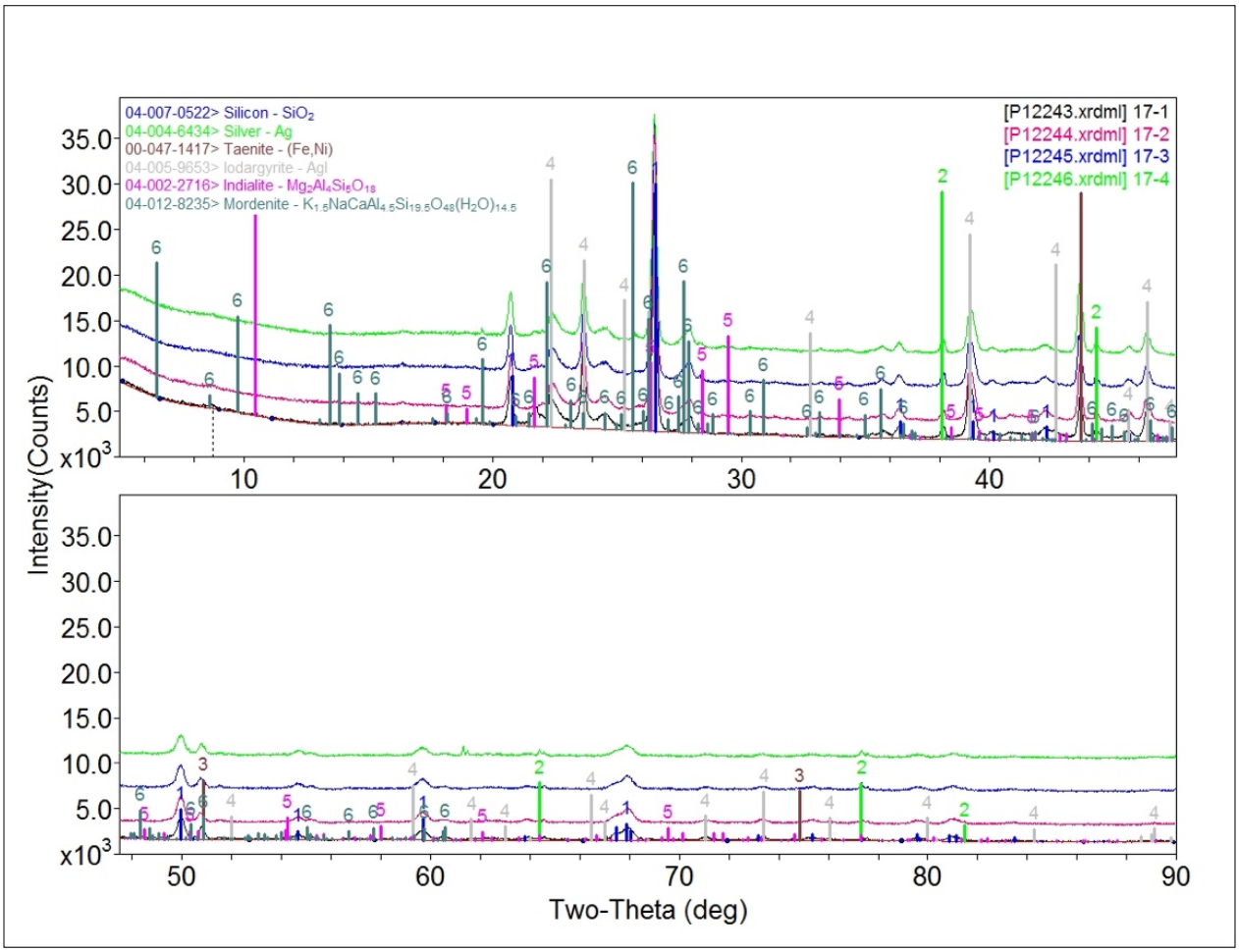

Figure B1. XRD patterns collected from samples 1–4.

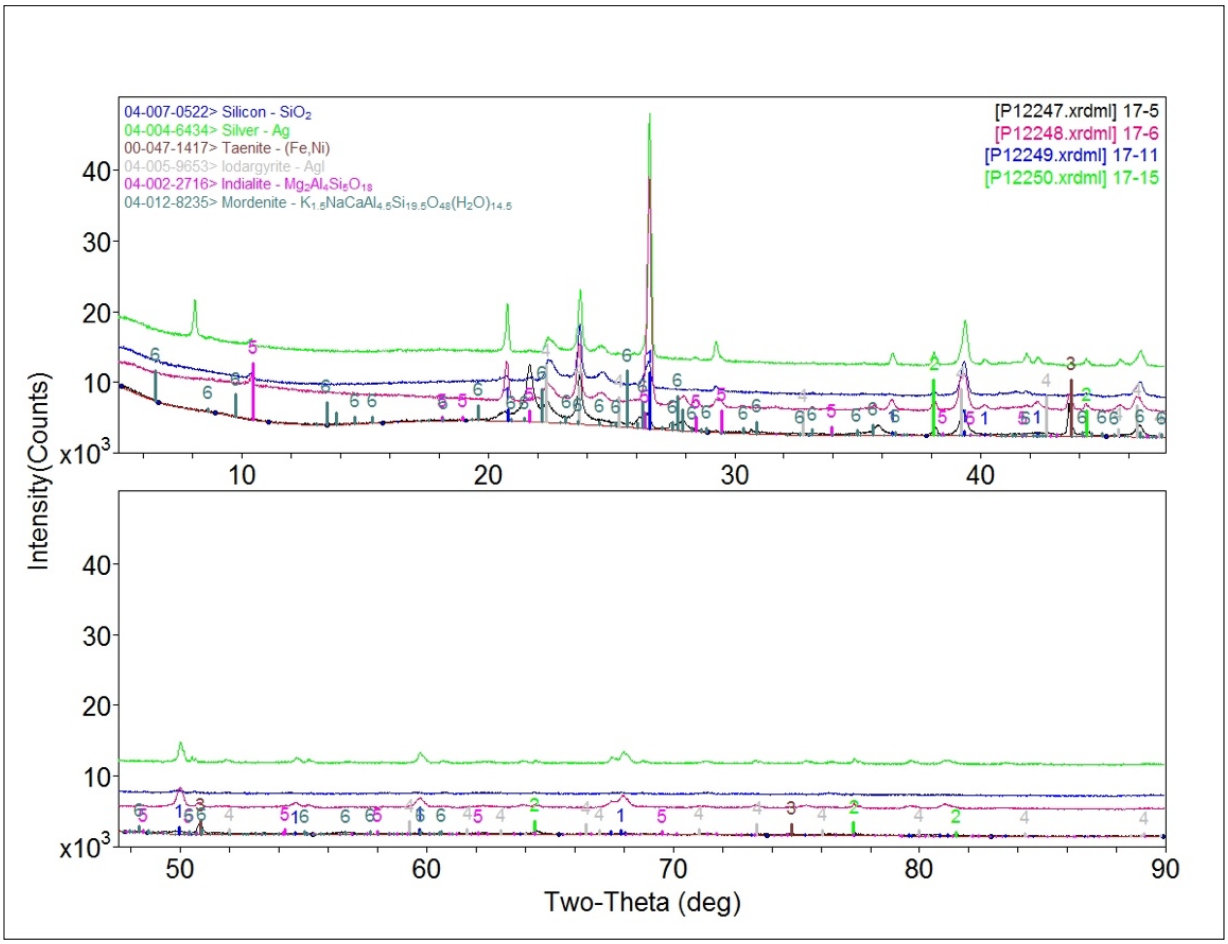

Figure B2. XRD patterns collected from samples 5, 6, 11, and 15.

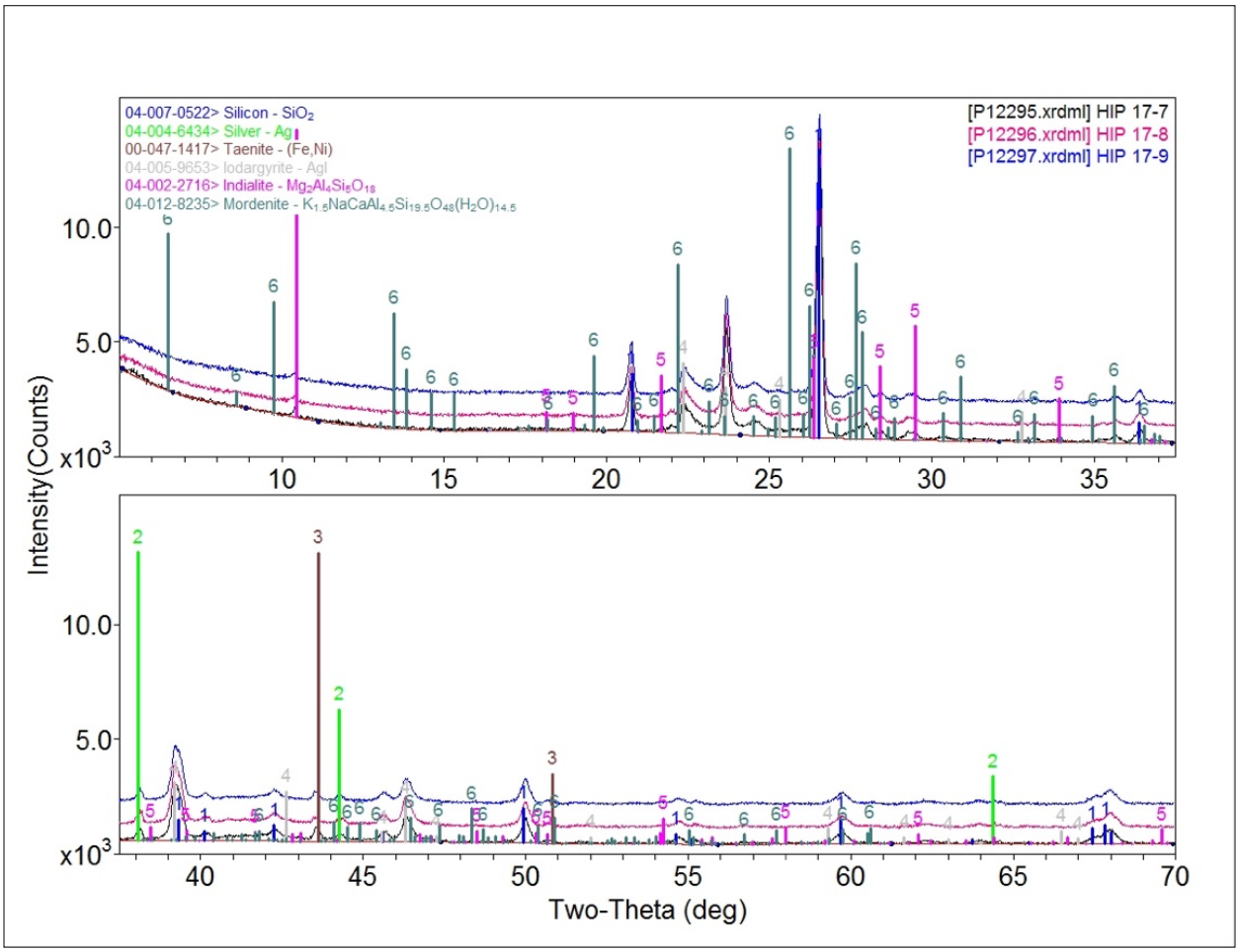

Figure B3. XRD patterns collected from samples 7–9.

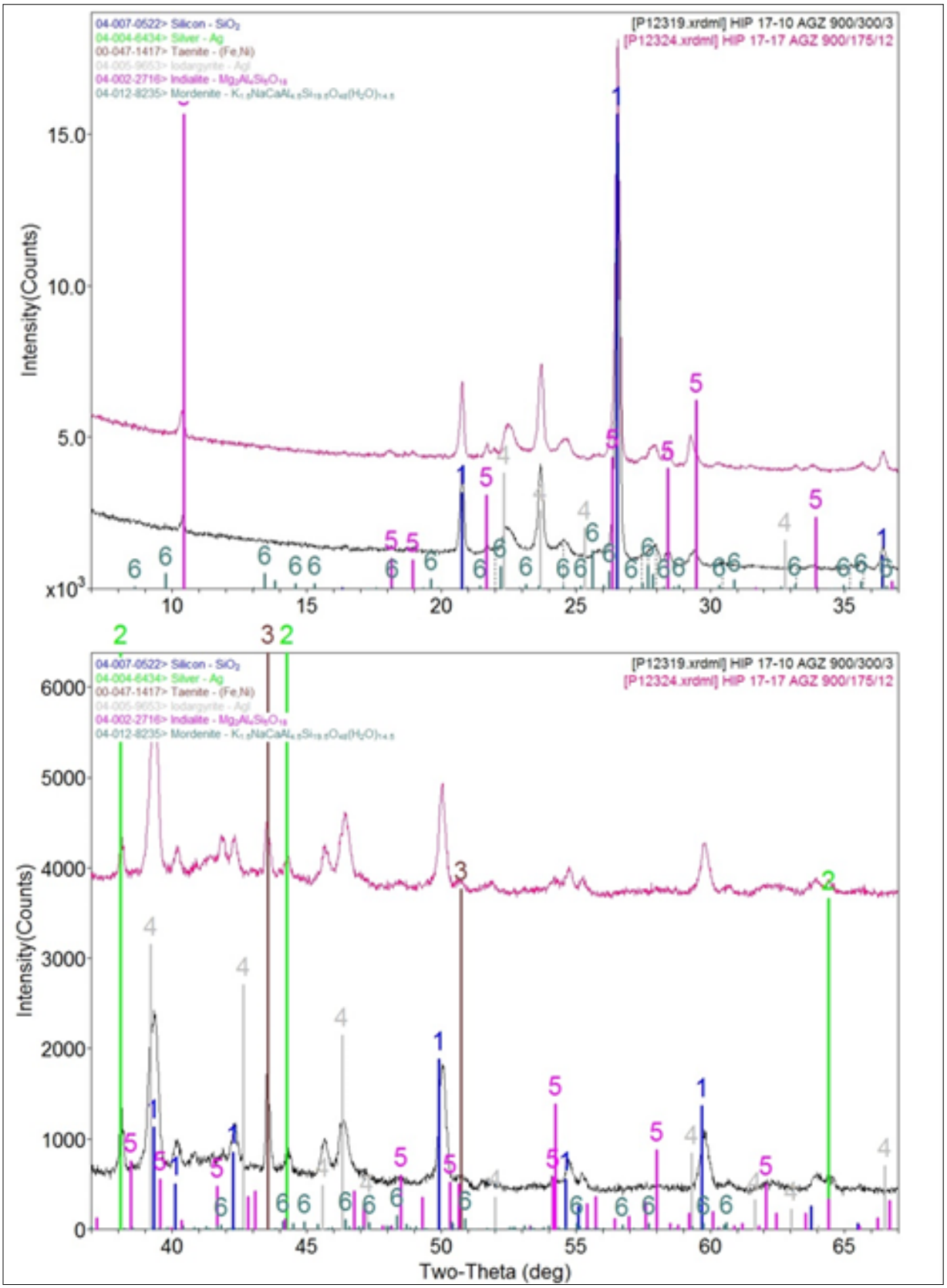

Figure B4. XRD patterns collected from samples 10 and 17.

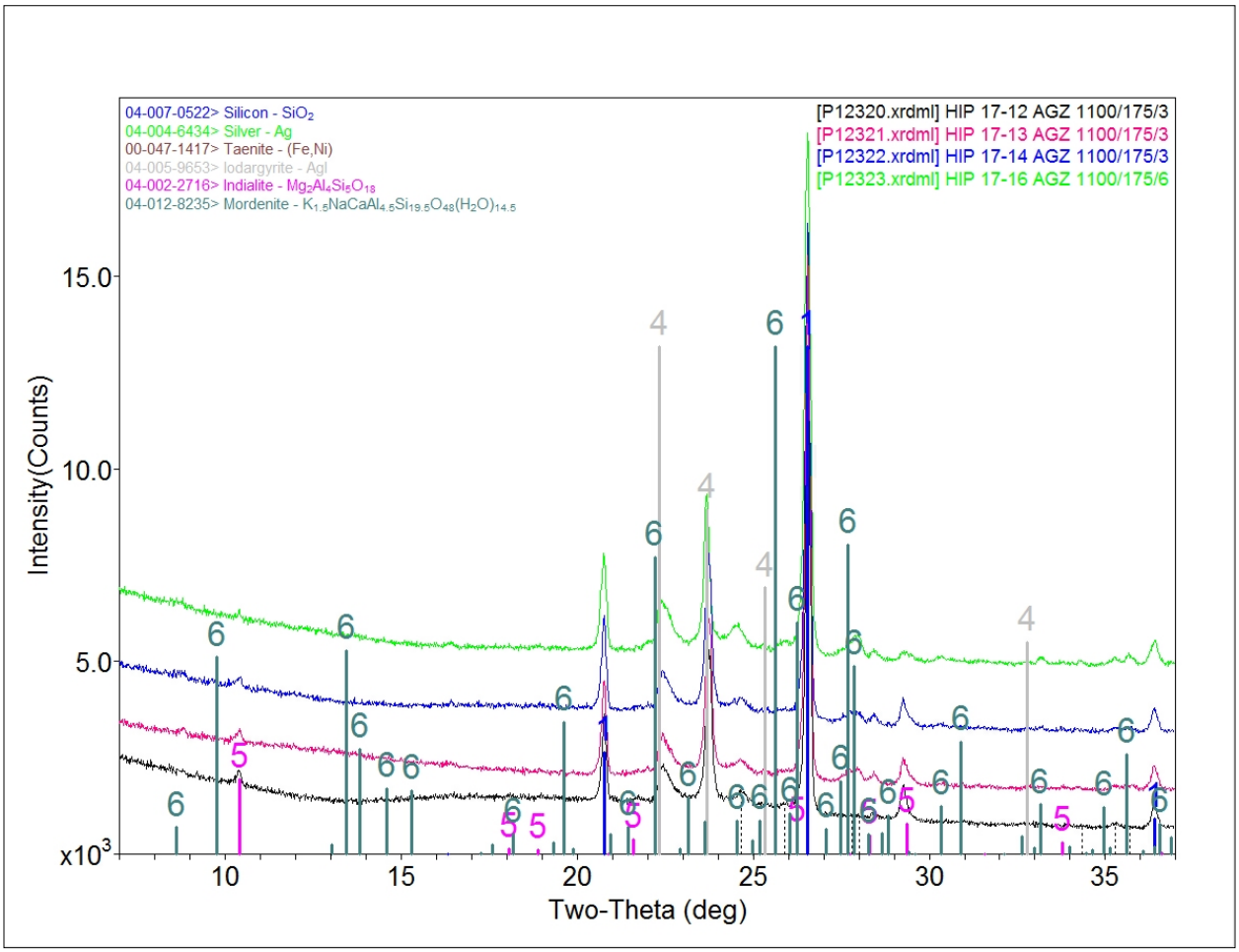

Figure B5. XRD patterns collected from samples 12–16.

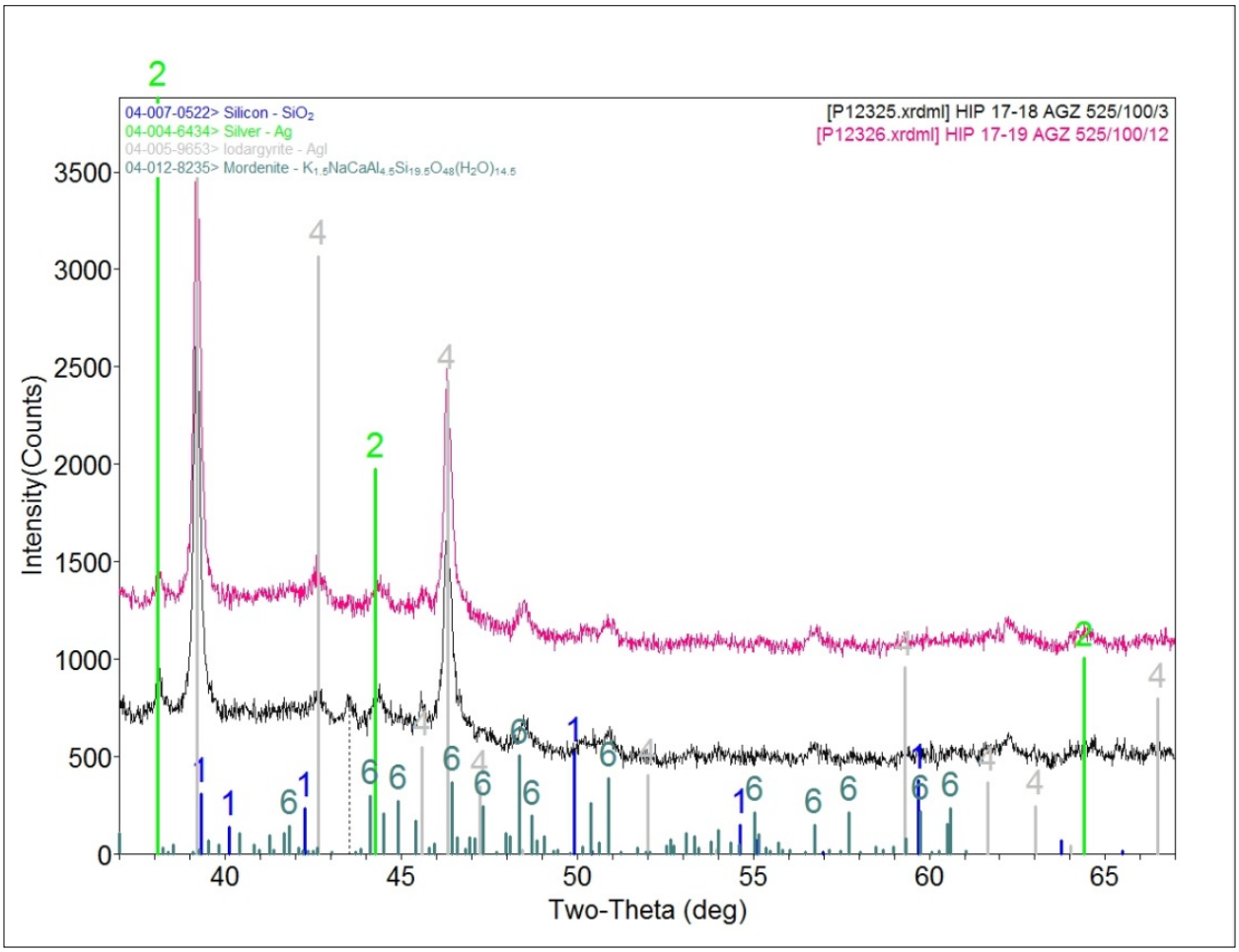

Figure B6. XRD patterns collected from samples 18 and 19.

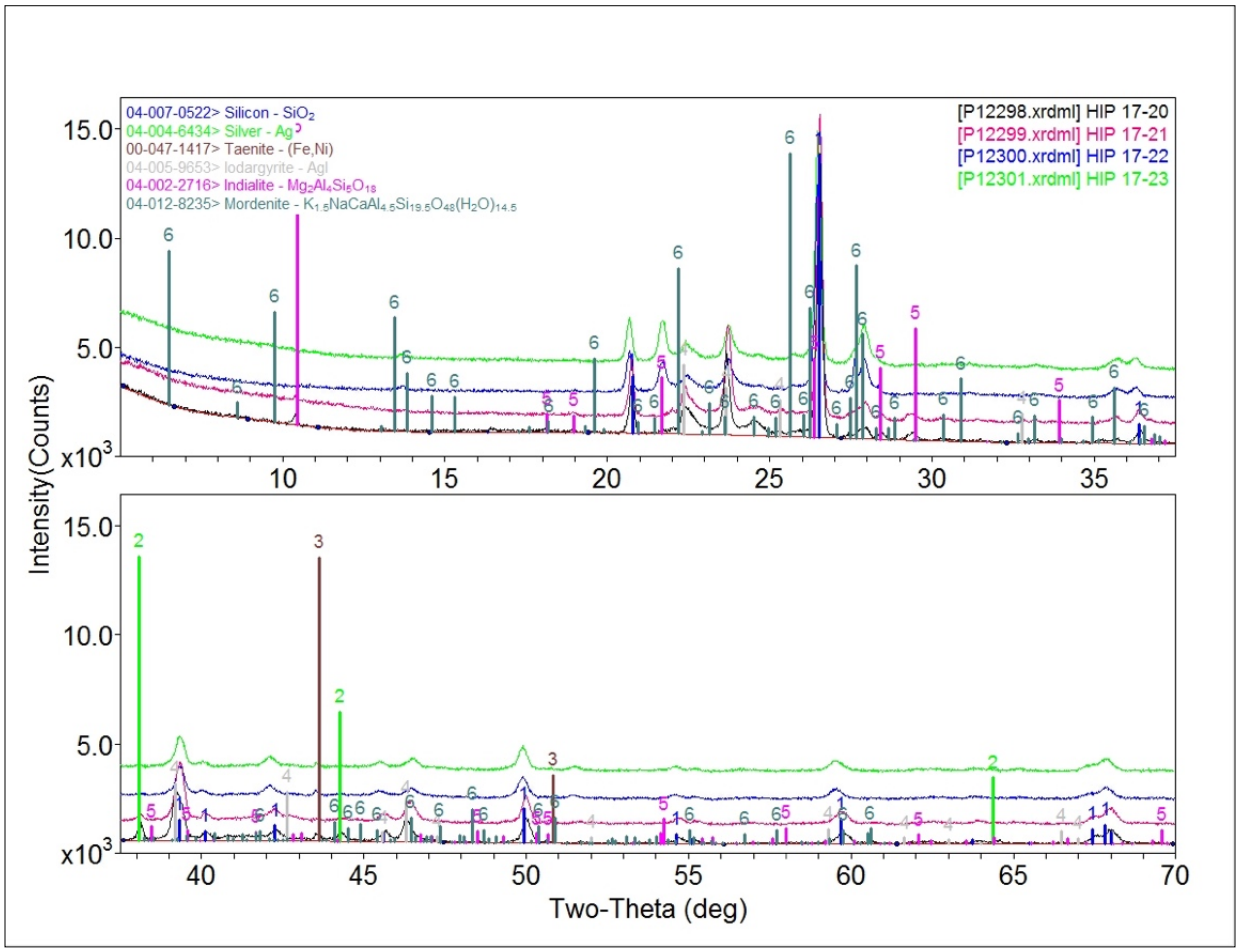

Figure B7. XRD patterns collected from samples 20–23.

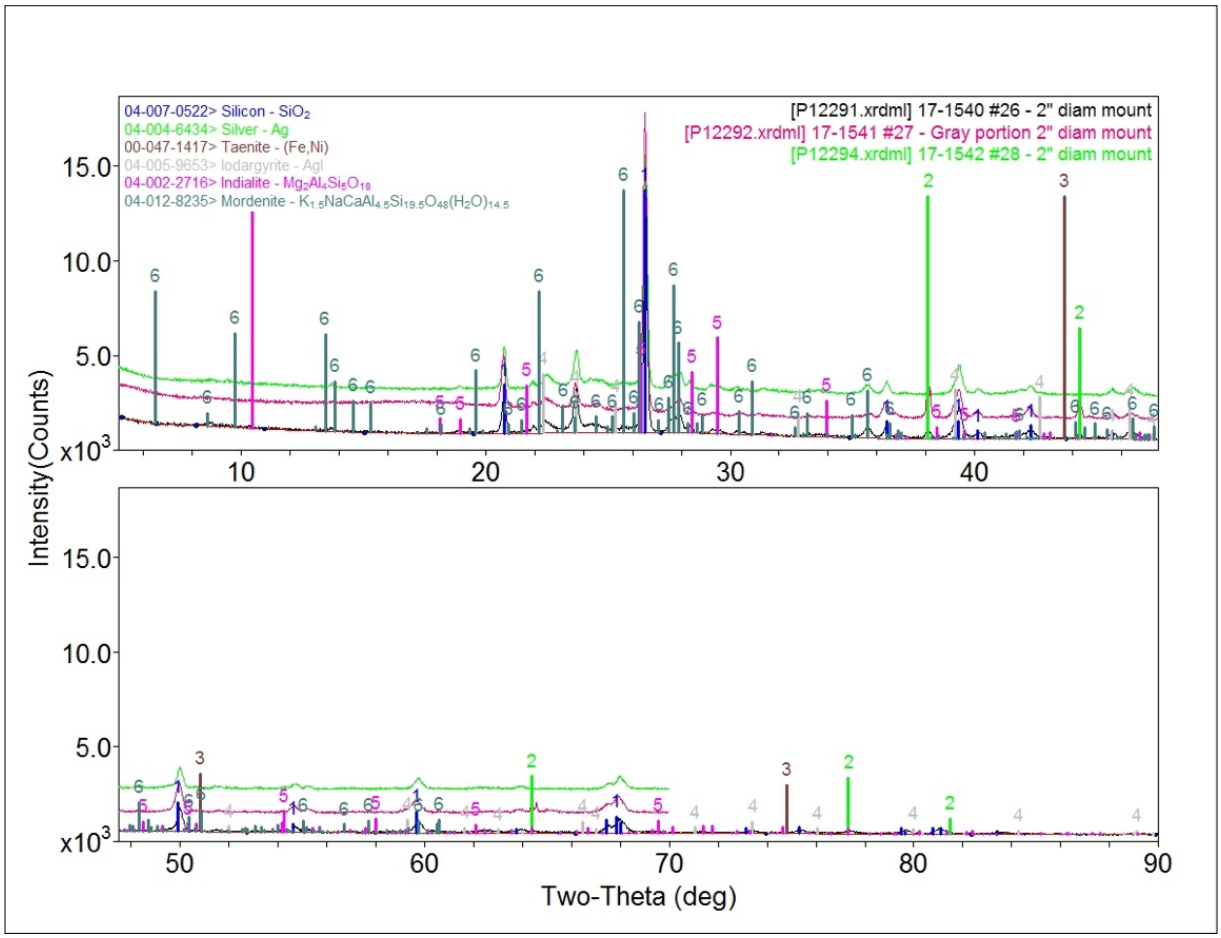

Figure B8. XRD patterns collected from samples 26–28.